



Multi-interacting global-change drivers reduce photosynthetic and resource use efficiencies and prompt a microzooplankton-phytoplankton uncoupling in estuarine communities

Marco J. Cabrerizo^{a,b,*} , Virginia E. Villafañe^{b,c}, E. Walter Helbling^b, Ricarda Blum^{b,c}, Juan I. Vizzo^{b,c}, Alejandro Gadda^{b,c,d}, Macarena S. Valiñas^{b,c}

^a Departamento de Ecología, Facultad de Ciencias, and Instituto Universitario de Investigación del Agua, Universidad de Granada, Campus de Fuentenueva s/n, 18071, Granada, Spain

^b Estación de Fotobiología Playa Unión (EFPU), Casilla de Correos 15, 9103, Rawson, Chubut, Argentina

^c Consejo Nacional de Investigaciones Científicas y Técnicas (CONICET), Argentina

^d Departamento de Biodiversidad y Biología Experimental, Facultad de Ciencias Exactas y Naturales, Universidad de Buenos Aires, C1428EGA, Buenos Aires, Argentina

ARTICLE INFO

Keywords:

Acidification
Carbon:chlorophyll *a* ratio
Electron transport rates
Grazing pressure
Gross primary production
Nutrient enrichment
Ultraviolet radiation
Warming

ABSTRACT

Plankton communities are subjected to multiple global change drivers; however, it is unknown how the interplay between them deviates from predictions based on single-driver studies, in particular when trophic interactions are explicitly considered. We investigated how simultaneous manipulation of temperature, pH, nutrient availability and solar radiation quality affects the carbon transfer from phytoplankton to herbivorous protists and their potential consequences for ecosystem functioning. Our results showed that multiple interacting global-change drivers reduced the photosynthetic (gross primary production-to-electron transport rates ratios, from 0.2 to 0.6–0.8) and resource use efficiencies (from 9 to 1 μg chlorophyll *a* (Chl *a*) $\mu\text{mol nitrogen}^{-1}$) and prompted uncoupling between microzooplankton grazing (*m*) and phytoplankton growth (μ) rates ($\mu > m$). The altered trophic interaction could be due to enhanced intra-guild predation or to microzooplankton growing at sub-optimal temperatures compared to their prey. Because phytoplankton-specific loss rates to consumers grazing are the most significant uncertainty in marine biogeochemical models, we stress the need for experimental approaches quantifying it accurately to avoid bias in predicting the impacts of global change on marine ecosystems.

1. Introduction

Greenhouse gas emissions and other anthropogenic activities are causing simultaneous alterations in several environmental drivers. The Intergovernmental Panel on Climate Change (IPCC et al., 2021) predicts, through different climate change scenarios, that the global sea surface temperature may increase between 1–6 °C and pH may decrease by 0.1–0.4 units by the year 2100. These rising temperatures at the ocean surface trigger, in some cases, a shoaling of the upper mixed layers and an increasing stratification of the water bodies. These phenomena can expose the organisms to higher levels of solar radiation, both ultraviolet (UVR) and photosynthetically active (PAR) radiation, in surface waters (Gao et al., 2012). In contrast, and as an opposing force, ongoing agricultural, urban, and industrial development is reducing the penetration

of solar radiation, thus decreasing UVR and PAR in the water column (Hintz et al., 2022), but also altering the biogeochemical cycles through nutrient runoffs (Herbert-Read et al., 2022). Consequently, marine organisms are being exposed to interactions among multiple global-change-related drivers (Côté et al., 2016). All these pressures on marine ecosystems threaten the structure and functioning of biological communities, trophic interactions, and ultimately, the provision of goods and services to humankind (Duarte, 2014; Hoegh-Guldberg and Bruno, 2010).

Microplankton (protists <200 μm) play a central role in marine food webs. On the one hand, phytoplankton generate ~50% of the total global primary production on Earth (Field et al., 1998); and on the other hand, microzooplankton remove ~70% of that production (Steinberg and Landry, 2017). While the characterization of the protist

* Corresponding author. Departamento de Ecología, Facultad de Ciencias, and Instituto Universitario de Investigación del Agua, Universidad de Granada, Campus de Fuentenueva s/n, 18071, Granada, Spain.

E-mail address: mjc@ugr.es (M.J. Cabrerizo).

<https://doi.org/10.1016/j.marenvres.2025.106952>

Received 4 June 2024; Received in revised form 24 December 2024; Accepted 6 January 2025

Available online 7 January 2025

0141-1136/© 2025 The Authors. Published by Elsevier Ltd. This is an open access article under the CC BY-NC license (<http://creativecommons.org/licenses/by-nc/4.0/>).

herbivorous-phytoplankton trophic interaction and its pivotal role in the carbon cycle has been well-stated for several decades ago (Calbet and Landry, 2004; Schmoker et al., 2013), we have scarce information on how global change is altering this interaction in natural plankton communities and what its consequences could be on higher trophic groups (i.e. mesozooplankton; Riebesell et al., 2018; Sommer et al., 2007). This is because few studies have evaluated such effects considering several drivers and different trophic levels at the same time. The available evidence shows that warming, nutrient availability and acidification combined favor the dominance of nano-over microphytoplankton species and benefit microzooplankton grazers, while impairing mesozooplankton (Duarte-Moreno et al., 2022). An enhanced microzooplanktonic link could potentially boost the energy transfer efficiency by shortening the length of the food web (Steinberg and Landry, 2017). Apart from this positive effect, other studies on coastal plankton communities have shown that global change conditions prompt shifts toward less palatable, bloom and chain-forming diatom communities (Anderson et al., 2022), along with reduced grazing by microzooplankton (Franzè et al., 2023). This response entails a reduced transference of energy and matter to higher trophic levels, and thus, most of it likely exported out of the euphotic zone. Moreover, the phytoplankton-specific loss rates to consumers grazing is the most significant uncertainty source in current marine biogeochemical models (Rohr et al., 2023), and trophic interactions amplify the cumulative effect of global change on marine ecosystems (Beauchesne et al., 2023). Therefore, employing experimental approaches becomes imperative to establish a baseline for such information and to avoid biased predictions regarding the impacts of global change.

The aim of this study is to quantify the potential impacts of multiple global change drivers on an estuarine plankton food web and their consequent effects on carbon flux towards higher trophic levels. We used an integrated multi-driver design in which the plankton communities were exposed to a future environmental condition, compared to current ones, of a temperature increase of +4 °C, a pH decrease of 0.4 units, and an abrupt pulse of inorganic macronutrients, both in presence and absence of microzooplankton. In addition, we investigated the role of solar UVR in mediating the impacts of the future environmental condition by exposing communities to two different solar radiation qualities: full solar radiation and only photosynthetically active radiation. Using this experimental approach, we quantified photosynthetic performance, oxygen evolution, taxonomic composition, resources use efficiency and the intrinsic phytoplankton growth rates (μ) and mortality rates (m) through consumption by microzooplankton over five days.

2. Material and methods

2.1. Study site, sampling and experimental setup

The Chubut river estuary is an ecosystem with median chlorophyll *a* (Chl *a*) concentrations ranging between ~30 (winter bloom period; July–August) and 3 (post- and pre-bloom periods; the rest of the year) $\mu\text{g L}^{-1}$. The increasing trend in Chl *a* towards the austral winter usually matches with a marked shift in the dominance of the communities such that the microphytoplankton contribution (%) to the total biomass is, on average, ~80% (July–August) and is mostly mediated by chain-forming diatoms (i.e. *Odontella aurita* and *Thalassiosira* sp.). During the rest of the year, microphytoplankton biomass accounts for ~20% and the community is mostly characterised by unidentified flagellates (Bermejo et al., 2018).

On August 30th 2022, a 100 L surface seawater sample (0.5 m, salinity >31) was collected during high tide at the mouth of the Chubut river (Egi station, 43° 20.5' S, 65° 3.25' W), using an acid-cleaned (1N HCl) bucket. The sample was pre-screened through a 200- μm mesh to eliminate mesozooplankton, put into acid-cleaned (1N HCl) plastic containers, and transported to the facilities of the Estación de Fotobiología Playa Unión (EPPU, 10 min away from the sampling site). Once in

the laboratory, 60 L of the original seawater containing the plankton community was distributed in 6 UVR-transparent 10 L microcosms (Low Density Polyethylene Cubitainers, Nalgene®, USA), and exposed to natural solar radiation outdoor for a period of five days, simulating both a Future environmental condition compared to a Control one, following a cluster design approach. We chose this approach because several global change drivers (e.g. temperature and pH) usually co-vary in nature (Boyd et al., 2010). The two environmental conditions (in triplicate; Fig. 1) were: (i) Control, in which the community was maintained as in the sampling condition (temperature = 8.8 ± 1 °C; pH = 8.19 ± 0.02), although with the addition of a pulse of nutrients as in the f/200 media (Guillard and Ryther, 1962), to ensure the community did not deplete nutrients during the incubation period; this resulted in an increase of 8.83, 0.36, and 1.06 $\mu\text{mol L}^{-1}$ of nitrate + nitrite, phosphate, and silicate, respectively; and (ii) Future, in which the community was exposed to increased temperature (+4 °C respect to Control) and acidification (7.82 ± 0.01), and a pulse of nutrients, as in the f/20 media, resulting in an increase of 88.3, 3.6, and 10.6 $\mu\text{mol L}^{-1}$ of nitrate + nitrite, phosphate, and silicate, respectively. The decrease in pH in the Future was achieved by the addition of CO_3^{2-} (as Na_2CO_3), HCO_3^- (as NaHCO_3) and HCl (0.1 N) to increase the pCO_2 and the dissolved inorganic carbon (DIC) (Gattuso et al., 2010), whereas the experimental warming was achieved by using a customized Arduino-controlled thermostatic bath. The nutrients pulses added in the Control and Future conditions simulate a low and a high discharges of the Chubut river, as daily occurs in the study area (Bermejo et al., 2018) or after extreme rainfall events (Vizzo et al., 2021), respectively. Temperature treatment simulated the mean intensity and duration of marine heatwave events found in the Southern Atlantic Ocean domain (Artana et al., 2024), whereas acidification mimicked the levels predicted in the last IPCC report for the year 2100 (RCP8.5 scenario; IPCC et al., 2021). We selected a five days experimental period for two reasons: (1) previous studies by our group in the study area have shown that this frame time is the minimum needed to detect changes in natural communities in response to global change drivers (Bermejo et al., 2020; Cabrerizo et al., 2018; Vizzo et al., 2021); and (2) to evaluate the overall metabolism and trophic interactions of the community during the phytoplankton exponential growth phase (see results section).

Daily and after the sunrise, 1.4 L subsamples were taken from each microcosm to prepare the treatments with presence (MZ_{100%}) and absence (MZ_{30%}) of microzooplankton (see description below) and to measure intrinsic phytoplankton growth (μ) and mortality (m), net community production (NCP) and respiration (CR) rates, and photosystem II performance (Fig. 1), as follows.

2.1.1. Microzooplankton grazing

Grazing was determined through the two-point modification dilution method using undiluted (100%; hereafter MZ_{100%}) and diluted (30%; hereafter MZ_{30%}) seawater. The validity of this approach, compared to the traditional multipoint dilution, has been demonstrated in several studies (Worden and Binder, 2003; Chen, 2015; Morison and Menden-Deuer, 2017). The dilution factor chosen based on previous results by Chen (2015) which showed that setting up a highly diluted water sample in a bottle yields net phytoplankton growth rates (k) comparable to intrinsic μ . For this purpose, 1 L of seawater was used as the MZ_{100%} treatment, with 500 mL allocated for t_0 (0 hs) samples and 500 mL for t_f (24 hs). Additionally, 300 mL was used to prepare the MZ_{30%} treatment, with 150 mL allocated for t_0 and 150 mL for t_f . Sterilised seawater (at 121 °C for 15 min) collected on the sampling day was used to dilute the samples in the MZ_{30%} treatment, with 350 mL per replicate. This dilution water used for the MZ_{30%} treatments was acidified (only for Future samples) and nutrient-enriched (for both conditions, as detailed in the experimental setup) prior to experimentation to maintain the pH and nutrient conditions. Once prepared, all samples were transferred into 500 mL narrow-mouth round translucent FEP bottles (Nalgene®, USA), incubated alongside the microcosms, and

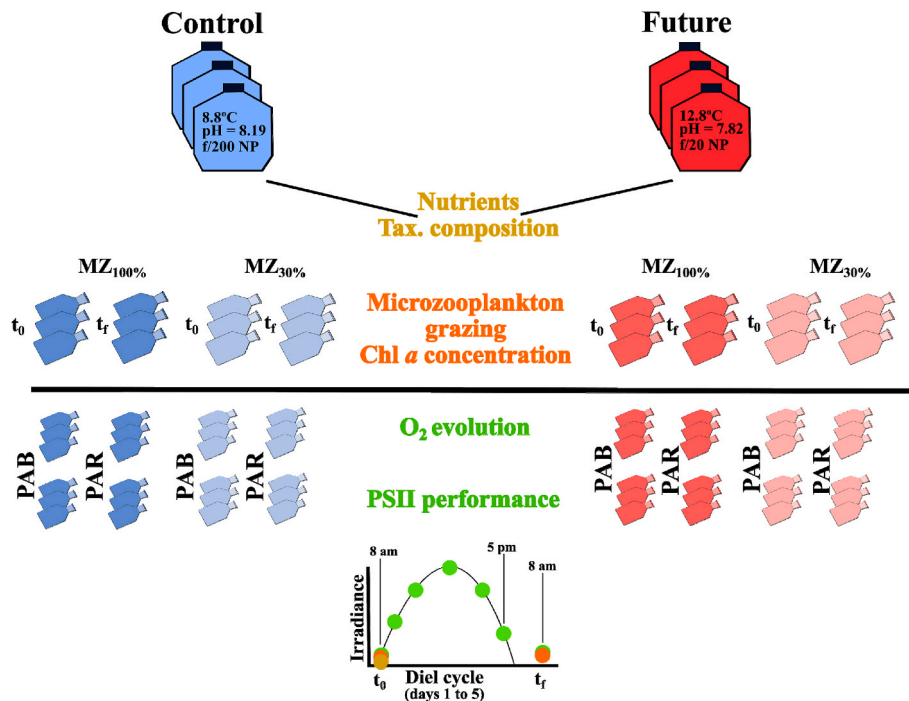


Fig. 1. - Graphical scheme of the cluster approach (Control vs. Future conditions) used to test the effects of acidification, nutrients, temperature, and ultraviolet radiation over diel cycles of oxygen evolution, photosystem II performance (PSII), and microzooplankton grazing pressure in estuarine plankton communities. PAB and PAR refer to the full spectrum of solar radiation and to only photosynthetically active radiation, respectively, MZ_{100%} and MZ_{30%} indicate the treatment either with presence or absence of microzooplankton, and t₀ and t_r are measurements performed at the beginning or after 24 h of incubation. Green (PSII and O₂ evolution), orange (microzooplankton grazing and chlorophyll *a*, Chl *a*), and yellow (nutrients and taxonomic composition) circles in the plot indicate when measurements were performed, and the bottles represent the replicates used in the experiment. (For interpretation of the references to colour in this figure legend, the reader is referred to the Web version of this article.)

exposed to solar radiation for 24 h. Samples for Chl *a* determination (see below) were collected when bottles were filled initially (t₀) and after 24 h (t_r). For this response variable, samples were exposed to the full spectrum of solar radiation. We did not distinguish between solar radiation quality treatments for taxonomic composition and microzooplankton grazing incubations (Fig. 1), as for NCP and CR and PSII performance, because it needs longer term scales that usually used to see any detectable effect by solar radiation in natural communities.

2.1.2. Net community production (NCP) and community respiration rates (CR) and PSII performance

For oxygen and PSII measurements, sub-samples of 50 mL were taken from the water prepared for microzooplankton grazing, placed in narrow-mouth round translucent 50-mL FEP bottles (Nalgene®, USA), and incubated next to the microzooplankton grazing samples for 24 h but under two radiation quality treatments, i.e. PAB (>280 nm, uncovered bottles) and PAR (>400 nm, bottles covered with UV 395 Opak Digepra film), i.e. a total of 48 bottles, 24 undiluted and 24 diluted (12 for PAB and 12 for PAR) for oxygen and PSII measurements (Fig. 1).

2.1.2.1. NCP and CR rates. Oxygen concentration was measured every 2 h during the solar day and then the following day before sunrise (7 measurements in total for each sample; Fig. 1) using a portable optode probe system (MiniOxy-10, Presens GmnH, Germany) equipped with optic fibers, and sensor-spots (SP-PSt3-NAU-D5-YOP) together with Oxyview 6.02 software to register the data. Before being used in the experimentation, the device was calibrated using a two-point (0 and 100% oxygen saturation) calibration together with temperature and atmospheric pressure data. In all samples, the photosynthetic dawn was identified as the oxygen concentration measured once the incubation started, after which all subsequent values were greater than it, while the photosynthetic dusk was defined as the maximum oxygen concentration

after which all subsequent values were lower (Bales and Nardi, 2007). Data from photosynthetic dawn were used to estimate NCP, whereas those from photosynthetic dusk were used to estimate CR.

2.1.2.2. PSII photochemical performance. Samples of 3 mL were taken from the 50-mL FEP bottles, and photosynthesis versus irradiance (P vs. E) curves were obtained with the same frequency as oxygen measurements (Fig. 1) by immediately exposing the samples to 9 steps of increasing irradiances, from 0 to 1350 μmol photons m⁻² s⁻¹, and measuring the effective photochemical quantum yield (Φ_{PSII}) in light-acclimated samples using a Pulse Amplitude Modulated (PAM) fluorometer (Water-ED PAM, Walz, Effeltrich, Germany).

We used the Φ_{PSII} values at the irradiance closer to the actual solar PAR at the time of measurements of the P vs. E curves to calculate the electron transport rates (ETR, in μmol e⁻ m⁻³ s⁻¹) as:

$$ETR = \Phi_{PSII} \times E_{PAR} \times \sigma \times 0.5$$

being E_{PAR} the PAR irradiance received by the community in the microcosms, σ the phytoplankton absorptivity (0.35 m⁻¹; mean absorption between 400 and 700 nm, as measured in the study area by our group (Helbling et al., 2023), and 0.5 is a correction factor, as it is considered that half of the light absorbed by cells is diverted to the PSII (Suggett et al., 2010).

Every day, during daylight hours, microcosms and incubation bottles for microzooplankton grazing, oxygen and PSII measurements were gently homogenised every 1–2 h to avoid cell settlement and to warrant homogenous irradiance inside them. At night, and to ensure that temperature conditions were maintained as during the solar day, microcosms were placed in temperature-controlled chambers, either Control or Future conditions, in darkness until the following day, when they were returned to the outdoor thermostatic incubators.

2.2. Counting and identification of plankton cells

Subsamples of 125 mL were collected at days one and five from each microcosm, placed in brown glass bottles, and fixed with buffered formalin (final concentration 0.4% of formaldehyde in the sample). We only took samples for phytoplankton identification at days one and five to be able to detect changes in the community composition. Subsamples of 10 mL were allowed to settle for 24 h in a sedimentation chamber (Hydro/Bios GmbH, Germany), and species were identified and enumerated (>2 μm i.e., nano- and microplankton) using an inverted microscope (Leica model DM IL, Germany) following the procedure by Villafañe and Reid (1995). A drop of Rose Bengal was added to the chamber to better distinguish small cells from detritus/sediment particles. The biovolume of cells was calculated by approximating the cell to the corresponding geometric figure (Hillebrand et al., 1999) and then converted into carbon (C) using the equations of Strathmann (1967).

2.3. Chlorophyll *a*

Samples of 200–250 mL from microzooplankton grazing incubations were filtered through Munktell MG-F glass fiber filters (25 mm diameter, Sweden) and placed in 15 mL centrifuge tubes with 5 mL of absolute methanol. Then, the samples were sonicated for 20 min at 20 °C, and the extraction was completed after 40 min more in darkness. After this period, the samples were centrifuged at 1500 rpm for 15 min, and the Chl *a* concentration was determined from fluorescence measurements (Turner Designs, model Trilogy, USA) using a standard procedure (Holm-Hansen and Riemann, 1978).

2.4. Solar radiation

Solar radiation was monitored using a European Light Dosimeter Network broadband filter radiometer (ELDONET, Real Time Computers, Germany) that measures UV-B (280–315 nm), UV-A (315–400 nm), and PAR (400–700 nm) every second, averages the data over a 1-min interval, and stores them in a computer. This radiometer, permanently installed on the roof of Estación de Fotobiología Playa Unión, is calibrated annually using a solar calibration procedure by comparing the irradiance data measured by the ELDONET in clear sky conditions with those obtained through the radiation transfer models STAR (Ruggaber et al., 1994) and Daylight (Björn and Murphy, 1985).

2.5. pH and nutrients

pH measurements in the microcosms were performed early in the morning on a daily basis using a pH meter (Ohaus, model ST300, USA). If necessary, pH was adjusted in the Future condition, through the acidification procedure described above to maintain the target pH values, as higher pH values can be attained due to photosynthesis (Villafañe et al., 2015).

Daily, subsamples of 100 mL for nitrate + nitrite, phosphate, and silicate determinations were collected from the microcosms, put in high-density polyethylene bottles and frozen (–20 °C) until analysis, which was performed with an autoanalyzer (Skalar model San Plus, USA).

2.6. Data analysis and calculations

Phytoplankton growth and mortality rates were estimated daily using the two-point modification of the dilution method (Anderson and Harvey, 2019; Menden-Deuer et al., 2018; Landry et al., 2022), as described above. Following Landry and Hassett (1982) and Chen (2015), phytoplankton growth rates (k) were calculated as follows:

$$k = \ln(\text{Chl}a_{t_f} / \text{Chl}a_{t_0}) / t$$

being $\text{Chl}a_{t_f}$ and $\text{Chl}a_{t_0}$ the Chl *a* concentrations measured at the end and

at the beginning of the incubation period, respectively, and t is the incubation period (24 h).

From both k in the MZ_{30%} and MZ_{100%} samples (i.e. k_{30} and k_{100}), we calculated the phytoplankton mortality rates (m) induced by grazing due to herbivorous protists as:

$$m = (k_{\text{MZ30\%}} - k_{\text{MZ100\%}}) / (1 - \times)$$

being \times the dilution factor used (30%).

We calculated the intrinsic phytoplankton growth rates (μ) as:

$$\mu = k_{\text{MZ100\%}} + m.$$

Finally, using the values of μ and m , we calculated the grazing pressure by microzooplankton ($m:\mu$ ratio), which is considered a proxy for the total biomass consumed by these heterotrophs.

The Chl *a* specific NCP and CR rates (in $\mu\text{mol O}_2 \mu\text{g Chl } a^{-1} \text{ h}^{-1}$) were calculated as the slope of the linear regression of oxygen concentrations versus time normalized by Chl *a* concentration. The Chl *a* specific ETR rates were calculated for each day and experimental condition integrating the area under the ETR versus time curve, and normalized by Chl *a* concentration. These daily rates were expressed hourly (in $\mu\text{mol e}^- \mu\text{g Chl } a^{-1} \text{ h}^{-1}$) by dividing them by the solar day (12 h). Gross primary production (GPP) rates were calculated as the sum of NCP and CR.

From the dissolved nitrate + nitrite (N) and phosphate (P) concentrations, we determined the N:P ratio in our experimental microcosms to assess potential nutrient limitations. The resource use efficiency (RUE) of the phytoplankton community was calculated as the ratio between the Chl *a* concentration (as a proxy of biomass) and the total dissolved resource for nitrogen (Ptacnik et al., 2008). The RUE of nitrogen (RUE_N), the limiting macronutrient in our case [N:P ratio (mol:mol) at the time of sampling = 3.08 ± 0.06], was used as a proxy for ecosystem functioning (Hodapp et al., 2019).

The C:Chl *a* ratio was calculated as the ratio between the total phytoplankton carbon biomass and Chl *a* concentration. From the GPP and ETR rates, we calculated the GPP:ETR ratio as a proxy for the community photosynthetic efficiency (i.e. the number of the oxygen released after the water splitting in the oxygen evolving complex due to solar radiation, and subsequently, the number of moles of electrons circulated through the PSII).

Repeated measures (RM) one-way analyses of variance (ANOVA) were used to test for significant differences between conditions (Control vs. Future) over time in the Chl *a* concentration, C:Chl *a* ratio, and total C biomass. RM three-way ANOVAs were used to test for significant differences between conditions, solar radiation quality (PAB and PAR only), and grazer treatment (100% and 30%) on NCP, CR, and ETR rates, as well as the GPP:ETR ratio. When the interactions were significant, a least significant differences (LSD) *post hoc* test was used to evaluate the differences between treatments. Linear and nonlinear regression analyses were used to evaluate the relationship between μ and m , and between the $m:\mu$ and Chl *a* or RUE_N , respectively. Student *t*-tests were used to determine significant differences between the $m:\mu$ vs. RUE_N slopes. Assumptions of normality (by Shapiro-Wilk's test) and homogeneity of variances (by Levene's or Mauchly tests) for ANOVA and RM-ANOVA, residual versus fitted value plots for regression analysis, and independence of the predictor variable respect to the explanatory one (by Pearson's correlation coefficient) were checked prior to using the ANOVA or regression analyses, respectively.

3. Results

3.1. Cellular composition and community structure

In terms of biomass, the phytoplankton community was dominated by microplanktonic species (between 84 and 92%, Fig. 2A), mainly centric diatoms (Fig. 2B). *Odontella aurita* and *O. mobiliensis* were prevalent at the beginning and at the end of the experiment in the

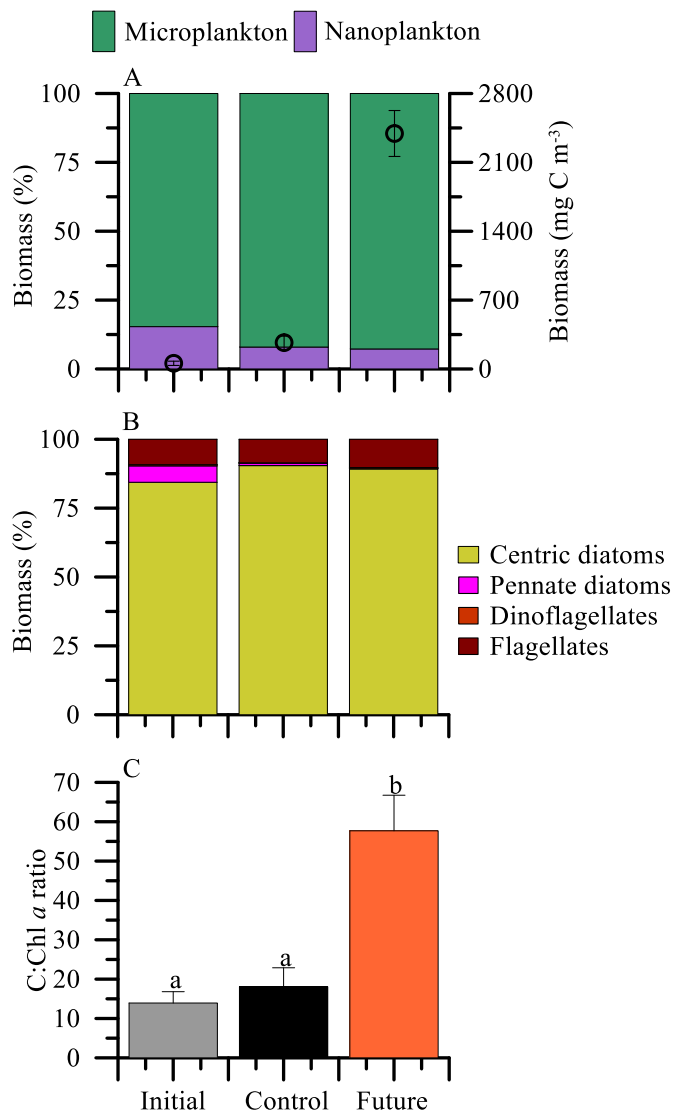


Fig. 2. Mean (\pm SD) contribution of micro- and nanophytoplankton to total carbon biomass (%) and total biomass (concentration, black circles) (A), contribution of the different taxonomic groups (B), and total carbon to chlorophyll *a* ratio (C) at the initial and at the end of the experimental period in plankton communities exposed to Control and Future environmental conditions. Letters on top of the bars represent significant differences by the Least Significant Differences *post hoc* test.

Control whereas *Thalassiosira* spp. (20–50 μ m in diameter) dominated at the end in the Future condition. Flagellates (mainly *Euglena* sp.) biomass at the end of the experiment was higher in the Future compared to both the Control condition and at the beginning of the experiment (182.50 vs. 22.81 and 5.10 mg C m⁻³, respectively), although their relative contribution to the total biomass was not significantly different between conditions (Fig. 2B). However, in terms of abundance, flagellates dominated the community at the initial time (\sim 62.92 \pm 6.95% of the total abundance; *data not shown*) whereas their contribution to the total abundance decreased under both Control and Future conditions at the end of the experimental period (\sim 36.83 \pm 7.88 vs. 18.10 \pm 4.74 % of the total abundance; *data not shown*). Although the proportion of the different size-class groups (%) was similar between conditions (Fig. 2A) in terms of biomass, their absolute values were significantly higher under Future > Control > Initial (black circles; LSD *post hoc* test, $p < 0.01$). The increases in biomass were coupled with significant (F -test = 349.61; $p < 0.0001$) variations in Chl *a* concentration, with concentrations ranging from 4.5 at day 1–14.9 and 41.3 μ g L⁻¹ at day 5 under

Control and Future conditions, respectively (Fig. 3A). Over the experimental period, the C:Chl *a* fluctuated between \sim 10 and 60, and this ratio was significantly higher under the Future condition compared to both the Control condition or at the beginning of the experiment (Fig. 2C).

This 6-fold increase in C:Chl *a* ratio matched with the growth experienced by centric diatoms after 5 days exposed to the Future condition (242.04 \pm 61.79 vs. 2195.26 \pm 137.70 mg C m⁻³); however, these changes were not translated into variations in the mean N:P ratio over the experimental period in this condition (Fig. 3B). By contrast, the N:P ratio fluctuated between 9.18 and 2.51 in the Control (Fig. 3B), primarily due to decreases in the mean concentrations of available N (from 12.41 \pm 0.05 to 2.15 \pm 0.10 μ M) over time.

3.2. Photochemical performance, metabolism, and photosynthetic efficiency

The evolution of oxygen concentrations and ETR cycles showed a characteristic hump-shaped pattern, with values being maxima at noon-early afternoon and minima at night (Fig. S1). The PAB treatment exerted a stimulatory effect on oxygen concentration evolution, compared with the PAR treatment, in the Control-MZ_{100%} treatment, but it was inhibitory in the Future-MZ_{30%} (Figs. S1A and B). ETR rates were similar in both conditions and regardless of the radiation treatment considered, except for days 1 and 3 in the Control-MZ_{30%} (Figs. S1C and D).

From oxygen evolution and PSII cycles showed above, we calculated the NCP, CR and ETR rates (Fig. 4). An interactive condition \times radiation \times grazer \times time effect was determined for all variables [NCP (F -test = 10.61, p -value < 0.0001), CR (F -test = 28.40, p -value < 0.0001), and ETR (F -test = 4.21, p -value < 0.01)] rates i.e. overall these rates were lower under Future, MZ_{100%} and PAB treatments than under Control, MZ_{30%} and PAR. NCP rates ranged between \sim 1 and \sim 4 μ mol O₂ μ g Chl *a*⁻¹ h⁻¹ over the experimental period, and they were significantly higher under the Future than the Control condition at day 1 and lower under the same conditions at days 4 and 5, particularly in samples exposed to the PAB treatment (Fig. 4A and B). CR rates ranged between \sim 0.5 and \sim 3 μ mol O₂ μ g Chl *a*⁻¹ h⁻¹, and they were significantly higher under the Control than under the Future condition in both MZ_{100%} and MZ_{30%} treatments (Fig. 4C and D). As consequence, GPP rates showed a similar response pattern to those of NCP and ranged between \sim 1 (Future) and \sim 2 (Control) and \sim 5 (in presence and absence of MZ) μ mol O₂ μ g Chl *a*⁻¹ h⁻¹ (Fig. S2). ETR rates ranged between \sim 2 and \sim 50 μ mol e⁻ μ g Chl *a*⁻¹ h⁻¹ and declined over the experimental period regardless of the condition, radiation quality, and MZ treatments (except for day 3 in the Control condition and with MZ_{30%}; Fig. 4E and F).

When evaluating the photosynthetic efficiency of the communities through the GPP:ETR ratio, we found an interactive condition \times

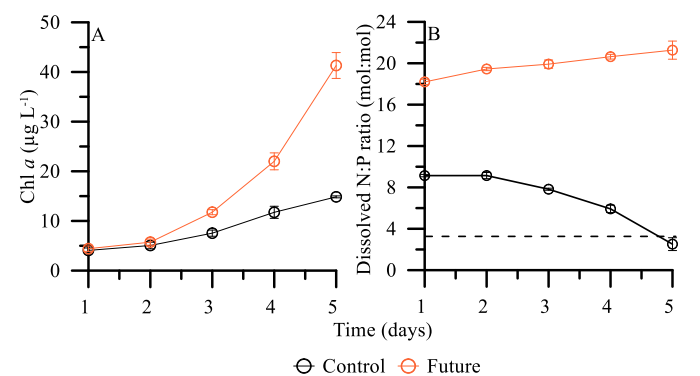


Fig. 3. Mean (\pm SD) chlorophyll *a* (Chl *a*) concentrations (A) and dissolved nitrogen to phosphorus ratios (N:P) (B) in plankton communities exposed to Control and Future environmental conditions over the experimental period. Dash line in panel B represents the N:P ratio at the sampling condition.

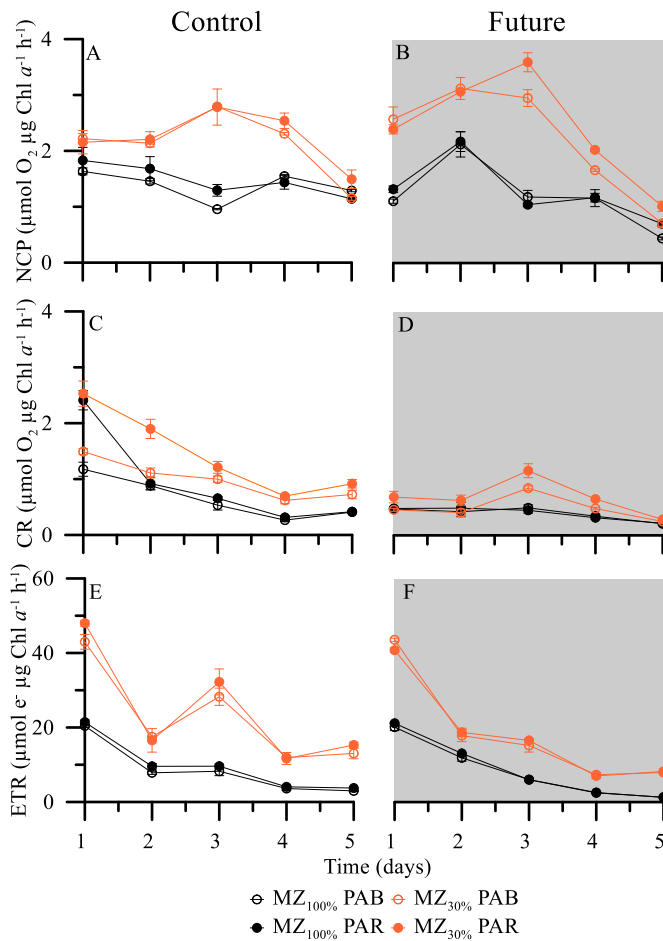


Fig. 4. Mean (\pm SD) net community production (A, B) (in $\mu\text{mol O}_2 \mu\text{g Chl a}^{-1} \text{h}^{-1}$), community respiration (C, D) (in $\mu\text{mol O}_2 \mu\text{g Chl a}^{-1} \text{h}^{-1}$), and electron transport (E, F) (in $\mu\text{mol e}^- \mu\text{g Chl a}^{-1} \text{h}^{-1}$) rates in plankton communities exposed to Control and Future environmental conditions under full spectrum of solar radiation (PAB) versus only photosynthetically active radiation (PAR), and in presence (MZ_{100%}) or absence (MZ_{30%}) of microzooplankton over the experimental period.

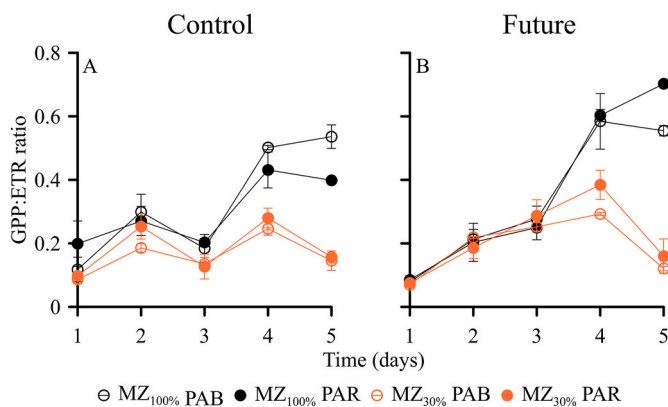


Fig. 5. Mean (\pm SD) ratio of gross primary production (GPP; in $\mu\text{mol O}_2 \mu\text{g Chl a}^{-1} \text{h}^{-1}$) to electron transport rates (ETR; in $\mu\text{mol e}^- \mu\text{g Chl a}^{-1} \text{h}^{-1}$) in plankton communities exposed to Control (A) and Future (B) environmental conditions under full spectrum of solar radiation (PAB) versus only photosynthetically active radiation (PAR), and in presence (MZ_{100%}) or (B) absence (MZ_{30%}) of microzooplankton over the experimental period. Higher GPP:ETR ratios indicate a lower photosynthetic efficiency, and vice versa.

radiation \times grazer \times time effect (F -test = 4.96, p -value < 0.001), with values ranging between 0.1 and 0.2 (MZ_{30%}) and \sim 0.8 (MZ_{100%}) over the experimental period (Fig. 5). GPP:ETR ratio values were significantly higher under the Future compared to the Control condition in the MZ_{100%} treatment on days 4 and 5 (LSD *post hoc* test, p < 0.05), whereas no clear effect of the Future condition occurred in the MZ_{30%} treatment (except day 3, where ratios were higher under a Future than a Control condition). Overall, these increasing ratios observed under a Future condition suggest a decrease in the photosynthetic efficiency of the plankton community, particularly under a Future environmental condition.

3.3. Microzooplankton-phytoplankton interaction: role of RUE_N and prey availability

Growth rates (μ) ranged between 0.15 and 1.2 d^{-1} and exceeded the total mortality (m) attributed to microzooplankton grazing, which ranged between ca. zero and 0.9 d^{-1} (Fig. 6A). The relationship between μ and m , as a measure of the trophic interaction strength, denoted an uncoupling (i.e. values below the 1:1 line) which attenuated over time under the Control condition ($R^2 = 0.90$, F -value (3) = 32.22, p -value < 0.01) but remained (or slightly accentuated) under the Future condition ($R^2 = 0.94$, F -value (3) = 57.57, p -value < 0.01). This weakened interaction, in particular under the Future, matched with μ rates 2-fold higher in this condition (0.46 ± 0.07 vs. 0.26 ± 0.05 d^{-1} ; t -Student test = -4.04, p = 0.01) as compared to the Control. The grazing pressure exerted by microzooplankton ($m:\mu$ ratio), as a proxy for total biomass consumed by grazers peaked at day 1, with >60% of the total produced by phytoplankton being consumed by grazers (Fig. 6B–S3A). In addition,

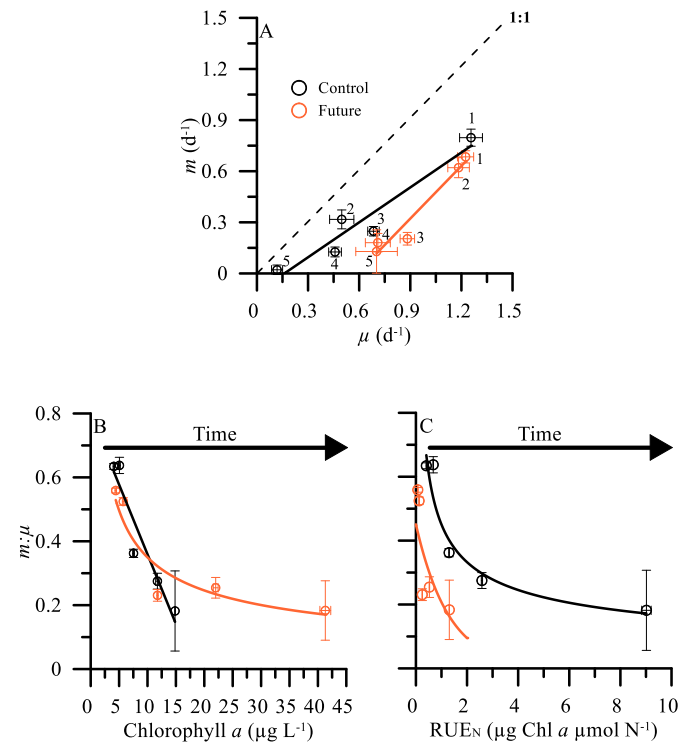


Fig. 6. Relationship between intrinsic phytoplankton growth (μ , in d^{-1}) and microzooplankton grazing (m , in d^{-1}) rates (A), microzooplankton grazing pressure ($m:\mu$ ratio) vs. chlorophyll a (in $\mu\text{g L}^{-1}$) (B), and vs. resource use efficiency of nitrogen (RUE_N , in $\mu\text{g Chl a} \mu\text{mol N}^{-1}$) (C) in plankton communities exposed to Control and Future environmental conditions over the experimental period. The dashed line represents the 1:1 m and μ relationship, the black and orange solid lines represent linear or non-linear fittings, and numbers close to the symbols represent the experimental day. (For interpretation of the references to colour in this figure legend, the reader is referred to the Web version of this article.)

while $m:\mu$ ratio decreased linearly with increasing Chl *a* concentrations under the Control ($R^2 = 0.88$, F -value₍₃₎ = 29.06, p -value = 0.01), this pattern was not maintained under the Future condition ($R^2 = 0.90$, F -value₍₃₎ = 6.10, p -value < 0.001). In fact, under the Future condition, we found a sustained $m:\mu$ ratio with Chl *a* concentrations >15 $\mu\text{g L}^{-1}$. At the end of the experimental period, the $m:\mu$ ratio remained ~ 0.3 irrespective of the condition, despite the prey availability (as Chl *a* concentration) being 3-fold higher under the Future compared to the Control condition (15 vs. 45 $\mu\text{g L}^{-1}$). This response pattern resembled that observed when assessing the relationship with the RUE_N , wherein grazing pressure decreased as resource efficiency increased (Fig. 6C–S3B; R^2 Control = 0.90 and R^2 Future = 0.82; $p < 0.01$), with the latter being significantly higher under Control than under the Future condition (Slope_{Control} = 0.45 ± 0.03 vs. Slope_{Future} = 0.17 ± 0.04 ; t -Student test = 9.70; $p = 0.0006$).

4. Discussion

This study shows that, over a short-term period, multiple interacting global-change drivers reduced the photosynthetic and resource use efficiencies within phytoplankton communities and prompted an uncoupling between the herbivorous protist and phytoplankton due to a weakening of the interaction strength (i.e. phytoplankton grew faster than consumed by microzooplankton). Despite a similar grazing pressure ($m:\mu$ ratio) exerted by microzooplankton, the amount of biomass (as Chl *a*) available was nearly threefold higher in the Future compared to the Control condition.

Our estimates of community production consumed ($m:\mu$ ratio, Fig. 6B and C) are lower than those documented in previous experimental (Horn et al., 2020; Menden-Deuer et al., 2018; Rose et al., 2009), and observational (Anderson and Harvey, 2019; Calbet and Landry, 2004; Schmoker et al., 2013) studies. However, these estimates are higher than those recently reported by Franzé et al. (2023) in a temperate estuarine ecosystem where no consumption by microzooplankton was detected when communities were simultaneously exposed to warming and a nutrient pulse. These authors attributed this response pattern to compositional shifts in the phytoplankton community towards less palatable species (i.e. large, colony and chain-forming diatoms) and enhanced phytoplankton growth rates. In our study, we did not observe a striking change in the taxonomic composition, as the biomass of microplanktonic chain-forming diatoms, such as *Thalassiosira* sp. and *O. aurita*, dominated the community, whereas the grazing pressure fluctuated between 0.2 and 0.6 (i.e. microzooplankton consumed between 20% and 60% of the total phytoplankton biomass generated) over the experimental period (Fig. 6B and C). These variations in grazing pressure may be attributed to grazing rates being more negatively affected than growth was over time regardless of the condition considered [i.e. reductions between 7- and 9-fold for m vs. 1.5- and 6-fold for μ in Future vs. Control] (Fig. 6A). By contrast, this differential impact on both rates cannot be attributed neither a bottle effect derived from the microcosms volume used nor the duration of the experiment, as recent results by Domingues et al. (2023) have demonstrated that the combination of small volumes and short time scales render accurate estimates of the plankton responses to abiotic and biotic drivers.

Two nonexclusive plausible explanations for the findings presented above could be enhanced intraguild predation or suboptimal growth temperatures for microzooplankton compared to phytoplankton. Regarding predation, we found that the proportion of flagellates, major contributors to grazing in coastal areas (Sherr and Sherr, 2007), was reduced by 43–60%. This observation aligns with the hypothesis that microzooplankton can regulate their own population (Nielsen and Kirboe, 1994; Paffenhöfer, 1998; Flynn et al., 2013) and with previous experimental findings, which evidenced that 79% of microzooplankton production is consumed by the microzooplankton (Franzé and Modigh, 2013). Regarding the second explanation, and according to the Metabolic Theory of Ecology predictions (Brown et al., 2004) and

experimental evidence (Chen et al., 2012; López-Urrutia et al., 2006; Rose and Caron, 2007), it is well-stated that the metabolism of heterotrophs, including microzooplankton grazing, increases faster than that of autotrophs (i.e. phytoplankton growth) due to their higher sensitivity (addressed as activation energy) to temperature increases. However, Liu et al. (2019) showed that, in coastal waters, the microzooplankton grazing rate has a range of optimal temperatures (T_{opt}) 3 °C higher than that of the phytoplankton growth rate. Therefore, it is plausible that our phytoplankton communities were closer to their T_{opt} than microzooplanktonic communities in the Future condition due to the 4 °C increase experienced; hence, the reductions observed in growth were lower than those observed in grazing.

It is worth mentioning that in our experimental approach the interaction of temperature with acidification, nutrients and solar radiation might have exerted a synergistic effect on the grazing rates. There is compelling evidence showing that these drivers, when acting individually, can directly (e.g. reducing the grazer growing rates, lowering the trophic coupling; Liu et al., 2023; López-Ábbate, 2021) and indirectly (e.g. reducing prey's nutritional quality; De Senerpont Domis et al., 2014; Johnson et al., 2022; Mitra and Flynn, 2005) influence consumers. We did not assess the stoichiometric composition of phytoplankton, but the C:Chl *a* ratio increased by 6-fold (Fig. 2C) and the RUE_N was ca. 5 times lower (Fig. 6C) in the Future condition compared to the initial and the Control conditions. This increase in the C:Chl *a* ratio entails a lower number of reaction centers available and a down-regulation of the light-harvesting complexes, which implies an increase in the amount of light required to saturate photosynthesis (Falkowski and Raven, 2007). This reasoning might be supported by the fact that communities experienced high-light availability (mean daily solar radiation conditions: PAR $\sim 700 \mu\text{mol photons m}^{-2} \text{s}^{-1}$; ultraviolet A and B, 53.74 and 0.61 W m^{-2} , respectively) during the experimental period. High-light conditions can potentially promote photoinhibition, hence a higher C:Chl *a* ratio is also considered an adaptive strategy to ameliorate photodamage (Raven and Samuelson, 1986). An indirect consequence of this is the cellular reallocation of resources to the dark reaction of photosynthesis and, ultimately, to the growth at the expense of the light-harvesting pigments. Other possible explanation for this response pattern could be the different thermal sensitivity of light and dark reactions (and catalysts associated with them) of photosynthesis, with the former being largely temperature-independent, and vice versa (Geider, 1987), or a down-regulation of carbon concentration mechanisms due to acidification (Giordano et al., 2005). In contrast, we do not find support that it was due to changes in species composition (see above) or a potential nutrient limitation. Previous observational and experimental studies have also reported that an increase in the C:Chl *a* ratio is a common strategy among phytoplankton growing under nutrient-limited conditions (Jakobsen and Markager, 2016; Marañón et al., 2018). Nevertheless, the N:P ratios and mean nutrient concentrations recorded during the incubations were slightly higher than those predicted by Redfield (1934). These findings suggest that phytoplankton could divert part of the consumed nitrogen to the synthesis of N-demanding processes and cell division, instead of pigments biosynthesis or other cellular organelles, thereby explaining the reduced RUE_N observed. This argumentation is additionally supported by the increased GPP:ETR ratios (i.e. reduced photosynthetic efficiency) observed when microzooplankton was present (Fig. 5). Thus, we speculate that all these changes could potentially have led to an increase in the C:nutrients ratio of the community, resulting in lower nutritional quality for preys under these conditions. Despite this, we did not find any support to the idea that a lowered food quality, along with stressful conditions, entails that consumers need a higher amount of prey to satisfy their energetic demands (Duarte-Moreno et al., 2022). Further studies quantifying how the interactions between multiple global-change drivers alter the microzooplankton grazing behavior could clarify the existing contradictory findings.

5. Conclusion

In summary, our study sheds light about how the interplay between multi-interacting global change drivers and biotic interactions impairs photosynthetic efficiency and modulates the availability of community production to other trophic levels. We acknowledge that our short-term incubations cannot fully replicate the complexity of natural conditions, in particular because the acclimation and adaptation responses of communities require longer temporal scales to operate than those considered here. However, these systems of intermediate complexity where many species interact, allow capturing indirect effects, shifts in the phytoplankton composition and feedbacks on the trophic energy transfer. Due to its strong environmental and ecological relevance, they are a mandatory tool for understanding the dynamics of trophic interactions and providing baseline information to empirical models. Finally, the alterations reported in the functioning of food webs and trophic interactions could promote the export of biomass out of the euphotic zone, fuelling bacterial decomposition and the benthic food web, but also could diminish the energy transfer efficiency to higher trophic levels. A decrease in the transfer efficiency of biomass could consequently reduce the high secondary production existing in the Patagonian area, including its fisheries.

CRedit authorship contribution statement

Marco J. Cabrerizo: Writing – original draft, Visualization, Validation, Methodology, Investigation, Formal analysis, Data curation, Conceptualization. **Virginia E. Villafañe:** Writing – review & editing, Visualization, Validation, Methodology, Investigation, Conceptualization. **E. Walter Helbling:** Writing – review & editing, Visualization, Validation, Methodology, Investigation, Conceptualization. **Ricarda Blum:** Writing – review & editing, Visualization, Validation, Methodology, Investigation, Conceptualization. **Juan I. Vizzo:** Writing – review & editing, Visualization, Validation, Methodology, Investigation, Conceptualization. **Alejandro Gadda:** Writing – review & editing, Visualization, Validation, Methodology, Investigation, Conceptualization. **Macarena S. Valiñas:** Writing – review & editing, Visualization, Validation, Supervision, Project administration, Methodology, Investigation, Funding acquisition, Formal analysis, Conceptualization.

Declaration of competing interest

The authors declare that they have no known competing financial interests or personal relationships that could have appeared to influence the work reported in this paper.

Acknowledgments

This work was supported by the Agencia Nacional de Promoción Científica y Tecnológica (ANPCyT, PICT2017-0411 and PICT2020-0972), the Cooperativa Eléctrica y de Servicios de Rawson, and Fundación Playa Unión. MJC was funded by a Captación, Incorporación y Movilidad de Capital Humano de I + D + i postdoctoral contract from Junta de Andalucía (POSTDOC-21-00044), by the Ramón y Cajal program (RYC2023-042504-I) and TITAN project (PID2022-136280NA-I00) from MCIN/AEI/10.13039/501100011033/ and European Regional Development Fund, and his visits at EFPU by PICT2017-0411 and PICT2020-0972 granted to MSV and VEV, respectively, and by Fundación Playa Unión. RB, JIV, and AG are funded by doctoral fellowships from Consejo Nacional de Investigaciones Científicas y Técnicas of Argentina (CONICET). Comments and suggestions by the Editor Julián Blasco and three anonymous reviewers are acknowledged. This is contribution no. 203 of Estación de Fotobiología Playa Unión. The authors declare that they have no known competing financial interests or personal relationships that could have influenced the work reported in this paper.

Appendix A. Supplementary data

Supplementary data to this article can be found online at <https://doi.org/10.1016/j.marenvres.2025.106952>.

Data availability

Data will be made available on request.

References

- Anderson, S.I., Franzè, G., Kling, J.D., Wilburn, P., Kremer, C.T., Menden-Deuer, S., et al., 2022. The interactive effects of temperature and nutrients on a spring phytoplankton community. *Limnol. Oceanogr.* 67, 634–645.
- Anderson, S.R., Harvey, E.L., 2019. Seasonal variability and drivers of microzooplankton grazing and phytoplankton growth in a subtropical estuary. *Front. Mar. Sci.* 6, 174.
- Artana, C., Rodrigues, R.R., Fevrier, J., Coll, M., 2024. Characteristics and drivers of marine heatwaves in the western South Atlantic. *Commun. Earth. Environ.* 5, 555.
- Bales, J.D., Nardi, M.D., 2007. Automated Routines for Calculating Whole-Stream Metabolism—Theoretical Background and User's Guide. U.S. Geological Survey Techniques and Methods. U. S. Department of Interior and U. S. Geological Survey, p. 33.
- Beauchesne, D., Cazelles, K., Daigle, R., Gravel, D., Archambault, P., 2023. Ecological interactions amplify cumulative effects in marine ecosystems. *Research Square*, preprint.
- Bermejo, P., Durán-Romero, C., Villafañe, V.E., Helbling, E.W., 2020. Influence of fluctuating irradiance on photosynthesis, growth and community structure of estuarine phytoplankton under increased nutrients and acidification. *J. Exp. Mar. Biol. Ecol.* 526.
- Bermejo, P., Helbling, E.W., Durán-Romero, C., Cabrerizo, M.J., Villafañe, V.E., 2018. Abiotic control of phytoplankton blooms in temperate coastal marine ecosystems: a case study in the South Atlantic Ocean. *Sci. Total Environ.* 612, 894–902.
- Björn, L.O., Murphy, T.M., 1985. Computer calculation of solar ultraviolet radiation at ground level. *Physiol. Veg.* 23, 555–561.
- Boyd, P.W., Strzepek, R., Fu, F.-X., Hutchins, D.A., 2010. Environmental control of open-ocean phytoplankton groups: now and in the future. *Limnol. Oceanogr.* 55, 1353–1376.
- Brown, J.P., Gillooly, F., Allen, A.P., Savage, V.M., West, G.B., 2004. Toward a metabolic theory of ecology. *Ecology* 85, 1771–1789.
- Cabrerizo, M.J., Carrillo, P., Villafañe, V.E., Medina-Sánchez, J.M., Helbling, E.W., 2018. Increased nutrients from aeolian-dust and riverine origin decrease the CO₂-sink capacity of coastal South Atlantic waters under UVR exposure. *Limnol. Oceanogr.* 63, 1191–1203.
- Calbet, A., Landry, M.R., 2004. Phytoplankton growth, microzooplankton grazing, and carbon cycling in marine systems. *Limnol. Oceanogr.* 49, 51–57.
- Côté, I.M., Darling, E.S., Brown, C.J., 2016. Interactions among ecosystems stressors and their importance in conservation. *Proc. R. Soc. Lond. B Biol. Sci.* 283, 20152592.
- Chen, B., 2015. Assessing the accuracy of the “two-point” dilution technique. *Limnol. Oceanogr. Methods* 13, 521–526.
- Chen, B., Landry, M.R., Huang, B., Liu, H., 2012. Does warming enhance the effect of microzooplankton grazing on marine phytoplankton in the ocean? *Limnol. Oceanogr.* 57, 519–526.
- De Senerpont Domis, L., Van de Waal, D.B., Helmsing, N.R., Van Donk, E., Mooij, W.M., 2014. Community stoichiometry in a changing world: combined effects of warming and eutrophication on phytoplankton dynamics. *Ecology* 95, 1485–1495.
- Domingues, R.B., Mosley, B.A., Nogueira, P., Maia, I.B., Barbosa, A.B., 2023. Duration, but not bottle volume, affects phytoplankton community structure and growth rates in microcosm experiments. *Water* 15, 372.
- Duarte-Moreno, H., Köring, M., Di Pane, J., Tremblay, N., Wiltshire, K.H., Boersma, M., et al., 2022. An integrated multiple driver mesocosm experiment reveals the effect of global change on planktonic food web structure. *Commun. Biol.* 5, 179.
- Duarte, C.M., 2014. Global change and the future ocean: a grand challenge for marine sciences. *Front. Mar. Sci.* 1, 1–16.
- Falkowski, P., Raven, J.A., 2007. *Aquatic Photosynthesis*. Princeton University Press, Princeton.
- Field, C.B., Behrenfeld, M.J., Randerson, J.T., Falkowski, P., 1998. Primary production of the Biosphere: integrating terrestrial and oceanic components. *Science* 281, 237–240.
- Flynn, K.J., Stoecker, D.K., Mitra, A., Raven, J.A., Glibert, P.M., Hansen, P.J., et al., 2013. Misuse of the phytoplankton-zooplankton dichotomy: the need to assign organisms as mixotrophs within plankton functional types. *J. Plankton Res.* 35, 3–11.
- Franzè, G., Anderson, S.I., Kling, J.D., Wilburn, P., Hutchins, D.A., Litchman, E., et al., 2023. Interactive effects of nutrients and temperature on herbivorous predation in a coastal plankton community. *Limnol. Oceanogr.* 68, S144–S157.
- Franzè, G., Modigh, M., 2013. Experimental evidence for internal predation in microzooplankton communities. *Mar. Biol.* 160, 3103–3112.
- Gao, K.S., Helbling, E.W., Häder, D.P., Hutchins, D.A., 2012. Responses of marine primary producers to interactions between ocean acidification, solar radiation, and warming. *Mar. Ecol. Prog. Ser.* 470, 167–189.
- Gattuso, J.P., Gao, K., Lee, K., Rost, B., Schulz, K.G., 2010. Approaches and tools to manipulate the carbonate chemistry. In: Riebesell, U., Fabry, V.J., Hansson, L., Gattuso, J.-P. (Eds.), *Guide to Best Practices for Ocean Acidification Research and Data Reporting*. Publications Office of the European Union, Brussels, pp. 41–52.

- Geider, R.J., 1987. Light and temperature dependence of the carbon to chlorophyll *a* in microalgae and cyanobacteria: implications for physiology and growth of phytoplankton. *New Phytol.* 106, 1–34.
- Giordano, M., Beardall, J., Raven, J.A., 2005. CO₂ concentrating mechanisms in algae: mechanisms, environmental modulation, and evolution. *Annu. Rev. Physiol.* 56, 99–131.
- Guillard, R.R.L., Ryther, J.H., 1962. Studies of marine planktonic diatoms. I. *Cyclotella nana* Husted, and *Detonula confervacea* (Cleve) gran. *Can. J. Microbiol.* 8, 229–239.
- Helbling, E.W., Banaszak, A.T., Valiñas, M.S., Vizzo, J.I., Villafañe, V.E., Cabrerizo, M.J., 2023. Browning, nutrient inputs, and fast vertical mixing from simulated extreme rainfall and wind stress alter estuarine phytoplankton productivity. *New Phytol.* 238, 1876–1888.
- Herbert-Read, J.E., Thornton, A., Amon, D.J., Birchenough, S.N.R., Côté, I.M., Dias, M.P., et al., 2022. A global horizon scan of issues impacting marine and coastal biodiversity conservation. *Nat. Ecol. Evol.* 6, 1262–1270.
- Hillebrand, H., Dürselen, C.D., Kirschtel, D., Pollinger, U., Zohary, T., 1999. Biovolume calculation for pelagic and benthic microalgae. *J. Phycol.* 35, 403–424.
- Hintz, N.H., Schulze, B., Wacker, A., Striebel, M., 2022. Ecological impacts of photosynthetic light harvesting in changing aquatic environments: a systematic literature map. *Ecol. Evol.* 12, e8753.
- Hodapp, D., Hillebrand, H., Striebel, M., 2019. "Unifying the concept of resource use efficiency in Ecology. *Front. Ecol. Evol.* 6, 00233.
- Hoegh-Guldberg, O., Bruno, J.F., 2010. The impact of climate change on the World's marine ecosystems. *Science* 328, 1523–1528.
- Holm-Hansen, O., Riemann, B., 1978. Chlorophyll *a* determination: Improvements in methodology. *Oikos* 30, 438–447.
- Horn, H.G., Boersma, M., Garzke, J., Sommer, U., Aberle, N., 2020. High CO₂ and warming affect microzooplankton food web dynamics in a Baltic Sea summer plankton community. *Mar. Biol.* 167, 69.
- IPCC, 2021. Summary for Policymakers. In: Masson-Delmotte, V., Zhai, P., Pirani, A., Connors, S.L., Péan, C., Berger, S. (Eds.), *Climate Change 2021: the Physical Science Basis. Contribution of Working Group I to the Sixth Assessment Report of the Intergovernmental Panel on Climate Change*, pp. 3–32 et al., editors, Cambridge, United Kingdom and New York, USA.
- Jakobsen, H.H., Markager, S., 2016. Carbon-to-chlorophyll ratio for phytoplankton in temperate coastal waters: Seasonal patterns and relationship to nutrients. *Limnol. Oceanogr.* 61, 1853–1868.
- Johnson, R., Langer, G., Rossi, S., Probert, I., Mammone, M., Ziveri, P., 2022. Nutritional response of a coccolithophore to changing pH and temperature. *Limnol. Oceanogr.* 67, 2309–2324.
- Landry, M.R., Hassett, R.P., 1982. Estimating the grazing impact of marine microzooplankton. *Mar. Biol.* 67, 283–288.
- Landry, M.R., Selph, K.E., Hood, R.R., Davies, C.H., Beckley, L.E., 2022. Low temperature sensitivity of picophytoplankton P : B ratios and growth rates across a natural 10°C temperature gradient in the oligotrophic Indian Ocean. *Limnol. Oceanogr.: Letters* 7, 112–121.
- Liu, K., Chen, B., Zhang, S., Sato, M., Shi, Z., Liu, H., 2019. Marine phytoplankton in subtropical coastal waters showing lower thermal sensitivity than microzooplankton. *Limnol. Oceanogr.* 64, 1103–1119.
- Liu, K., Nishioka, J., Chen, B., Suzuki, K., Cheung, S., Lu, Y., et al., 2023. Role of nutrients and temperature in shaping distinct summer phytoplankton and microzooplankton population dynamics in the western North Pacific and Bering Sea. *Limnol. Oceanogr.* 68, 649–665.
- López-Ábbate, M.C., 2021. Microzooplankton communities in a changing ocean: a risk assessment. *Diversity* 13, 82.
- López-Urrutia, A., San Martín, E., Harris, R.P., Irigoien, X., 2006. Scaling the Metabolic Balance of the Oceans, 103. *Proc. Natl. Acad. Sci. USA*, pp. 8739–8744.
- Marañón, E., Lorenzo, M.P., Cermeño, P., Mouriño-Carballido, B., 2018. Nutrient limitation suppresses the temperature dependence of phytoplankton metabolic rates. *ISME J.* 12, 1836–1845.
- Menden-Deuer, S., Lawrence, C., Franzè, G., 2018. Herbivorous protist growth and grazing rates at in situ and artificially elevated temperatures during an Arctic phytoplankton spring bloom. *PeerJ* 6, e5264.
- Mitra, A., Flynn, K.J., 2005. Predator–prey interactions: is 'ecological stoichiometry' sufficient when good food goes bad? *J. Plankton Res.* 27, 393–399.
- Morison, F., Menden-Deuer, S., 2017. Doing more with less?: Balancing sampling resolution and effort in measurements of protistan growth and grazing-rates. *Limnol. Oceanogr. Methods* 15, 794–809.
- Nielsen, T.G., Kirboe, T., 1994. Regulation of zooplankton biomass and production in a temperate, coastal ecosystem. 2. Ciliates. *Limnol. Oceanogr.* 39, 508–519.
- Paffenhöfer, G.-A., 1998. Heterotrophic protozoa and small metazoa: feeding rates and prey-consumer interactions. *J. Plankton Res.* 20, 121–133.
- Ptácnik, R., Solimini, A.G., Andersen, T., Tamminen, T., Brettum, P., Lepistö, L., et al., 2008. Diversity Predicts Stability and Resource Use Efficiency in Natural Phytoplankton Communities, vol. 105. *Proc. Natl. Acad. Sci. USA*, pp. 5134–5138.
- Redfield, A., 1934. On the proportions of organic derivatives in sea water and their relation to the composition of plankton. In: Daniel, R.J. (Ed.), *James Johnstone Memorial Volume*, pp. 177–192.
- Raven, J.A., Samuelson, G., 1986. Repair of photoinhibitory damage in *Anacystis nidulans* 625 (*Synechococcus* 6301); Relation to catalytic capacity for, and energy supply to, protein synthesis, and implications for μ_{max} and the efficiency of light-limited growth. *New Phytol.* 103, 625–643.
- Riebesell, U., Aberle-Malzahn, N., Achterberg, E.P., Algueró-Muñiz, M., Álvarez-Fernández, S., Aristegui, J., Bach, L.T., Boersma, M., Boxhammer, T., Guan, W., Haunost, M., Horn, H.G., Löscher, C.R., Ludwig, A., Spisla, C., Swat, M., Stange, P., Taucher, J., 2018. Toxic algal bloom induced by ocean acidification disrupts the pelagic food web. *Nat. Clim. Change* 8, 1082–1086.
- Rohr, T., Richardson, A.J., Lenton, A., Chamberlain, M.A., Shadwick, E.H., 2023. Zooplankton grazing is the largest source of uncertainty for marine carbon cycling in CMIP6 models. *Commun. Earth Environ.* 4, 212.
- Rose, J.M., Caron, D.A., 2007. Does low temperature constrain the growth rates of heterotrophic protists? Evidence and implications for algal blooms in cold waters. *Limnol. Oceanogr.* 52, 886–895.
- Rose, J.M., Feng, Y., Gobler, C.J., Gutiérrez, R., Hare, C.E., Leblanc, K., et al., 2009. Effects of increased pCO₂ and temperature on the North Atlantic spring bloom. II. Microzooplankton abundance and grazing. *Mar. Ecol. Prog. Ser.* 388, 27–40.
- Ruggaber, A., Dlugi, R., Nakajima, T., 1994. Modelling of radiation quantities and photolysis frequencies in the troposphere. *J. Atmos. Chem.* 18, 171–210.
- Schmoker, C., Hernández-León, S., Calbet, A., 2013. Microzooplankton grazing in the oceans: impacts, data variability, knowledge gaps and future directions. *J. Plankton Res.* 35, 691–706.
- Sherr, E.B., Sherr, B.F., 2007. Heterotrophic dinoflagellates: a significant component of microzooplankton biomass and major grazers of diatoms in the sea. *Mar. Ecol. Prog. Ser.* 352, 187–197.
- Sommer, U., Aberle, N., Engel, A., Hansen, T., Lengfellner, K., Sandow, M., et al., 2007. An indoor mesocosm system to study the effect of climate change on the late winter and spring succession of Baltic Sea phyto- and zooplankton. *Oecologia* 150, 655–667.
- Steinberg, D.K., Landry, M.R., 2017. Zooplankton and the ocean carbon cycle. *Ann. Rev. Mar. Sci.* 9, 413–444.
- Strathmann, R.R., 1967. Estimating the organic carbon content of phytoplankton from cell volume or plasma volume. *Limnol. Oceanogr.* 12, 411–418.
- Suggett, D.J., Oxborough, K., Baker, N.R., MacIntyre, H.L., Kana, T.M., Geider, R.J., 2010. Fast repetition rate and pulse amplitude modulation chlorophyll *a* fluorescence measurements for assessment of photosynthetic electron transport in marine phytoplankton. *Eur. J. Phycol.* 38, 371–384.
- Villafañe, V.E., Reid, F.M.H., 1995. Métodos de microscopía para la cuantificación del fitoplancton. In: Alveal, K., Ferrario, M.E., Oliveira, E.C., Sar, E. (Eds.), *Manual de Métodos Ficológicos*, pp. 169–185. Universidad de Concepción, Concepción, Chile.
- Villafañe, V.E., Valiñas, M.S., Cabrerizo, M.J., Helbling, E.W., 2015. Physio-ecological responses of Patagonian coastal marine phytoplankton in a scenario of global change: role of acidification, nutrients and solar UVR. *Mar. Chem.* 177, 411–420.
- Vizzo, J.I., Cabrerizo, M.J., Helbling, E.W., Villafañe, V.E., 2021. Extreme and gradual rainfall effects on winter and summer estuarine phytoplankton communities from Patagonia (Argentina). *Mar. Environ. Res.* 163, 105235.
- Worden, A.Z., Binder, B.J., 2003. Application of dilution experiments for measuring growth and mortality rates among *Prochlorococcus* and *Synechococcus* populations in oligotrophic environments. *Aquat. Microb. Ecol.* 30, 159–174.